Experimental verification of nonconstant potential and density on magnetic surfaces of helical nonneutral plasmas

H. Himura[a)] and H. Wakabayashi
The University of Tokyo, School of Frontier Sciences, Tokyo 113-0033, Japan

Y. Yamamoto
Department of Electronics, Kyoto Institute of Technology, Kyoto 606-8585, Japan

M. Isobe, S. Okamura, and K. Matsuoka
National Institute for Fusion Sciences, Gifu 509-5292, Japan

A. Sanpei and S. Masamune
Department of Electronics, Kyoto Institute of Technology, Kyoto 606-8585, Japan

(Received 7 July 2006; accepted 11 January 2007; published online 28 February 2007)

For the first time, nonconstant space potential ϕ_s and electron density n_e on magnetic surfaces of helical nonneutral plasmas are observed experimentally. The variation of ϕ_s grows with increasing electron injection energy, implying that thermal effects are important when considering the force balance along magnetic field lines. These observations confirm the existence of plasma equilibrium having nonconstant ϕ_s and n_e on magnetic surfaces of helical nonneutral plasmas. © *2007 American Institute of Physics*. [DOI: 10.1063/1.2458548]

I. INTRODUCTION

The magnetic surface is one of the most important and fundamental concepts in toroidal plasma confinement devices such as tokamaks[1] and stellarators.[2] In quasineutral plasmas, physical parameters such as pressure and space potential ϕ_s are in general thought to be constant on a magnetic surface. Irregularity of density is rapidly smoothed out along the magnetic field line of force. Variations in ϕ_s on the magnetic surface are also smoothed out or Debye shielded on distances shorter than 0.1 mm (typically for electron density $n_e \sim 10^{19}$ m^{-3} and electron temperature $T_e \sim 1$ keV). Thus, many analyses of such plasma equilibria have been performed by assuming that those physical parameters are magnetic surface quantities. However, this assumption is not always justified for toroidal plasmas.

There are one species[3] or electrically nonneutral plasmas[4] having a strong self-electric field. In recent years, these plasmas have been studied intensively as the basis for a variety of applications, such as the simultaneous confinement of multiple species of charged particles[5] and the confinement of antimatter particles,[6] and as a method of producing a fast perpendicular flow of ions.[4] Among others, toroidal traps of charged particles have an attractive benefit because they do not need the pair of electric barriers to confine charged particles like those in the Penning trap. In particular, in the helical trap[7,8] with magnetic surfaces, charged particles can be injected into the magnetic surfaces through the magnetic stochastic layer outside the last closed flux surface (LCFS).[7] This property allows the trap to be operated in steady state without tearing magnetic surfaces, contrary to the operation of other toroidal traps[5,9] for which an electron gun (henceforth, called e-gun) must unavoidably be inserted into the confinement region.

In the equilibrium state of one-species (pure electron) plasmas on magnetic surfaces, the force balance equation of the electron fluid is written as $m_e n_e (\vec{v}_e \cdot \nabla)\vec{v}_e = -en_e\vec{v}_e \times \vec{B} + en_e \nabla \phi_s - \nabla p_e$, where m_e, v_e, and p_e stand for the electron mass, velocity field, and pressure of the electron fluid, respectively. When n_e is far below the Brillouin density limit[3] $n_B = e_0 B^2/2m_e$, the convective term on the left-hand side can be ignored. In addition, when the plasma is assumed to be cold ($T_e = 0$), the ∇p_e term also vanishes. In that case, the force balance equation takes on the simple form of $\vec{v}_e \times \vec{B} = \nabla \phi_s$, which leads to $\vec{B} \cdot \nabla \phi_s = 0$. This means that ϕ_s must be constant along magnetic field lines of force; that is, on the magnetic surfaces.

However, when T_e is finite and p_e is relatively low, that is not the case. In this case, we must consider the parallel component of the force balance that is written as

$$en_e \nabla_{\parallel} \phi_s (= - en_e E_{//}) = \nabla_{\parallel} p_e, \tag{1}$$

where $\nabla_{//}$ represents the derivative along the magnetic field line of force. Assuming that T_e is constant on each magnetic surface, that is, T_e is a function of magnetic flux Ψ, Eq. (1) can be rewritten as

$$en_e \nabla_{\parallel} \phi_s (= - en_e E_{//}) = T_e(\Psi) \nabla_{\parallel} n_e. \tag{2}$$

Equation (2) can be integrated and has the solution $n_e \sim \exp(e\phi_s / T_e(\Psi))$ if n_e need not be constant along the magnetic field line of force. On the other hand, ϕ_s and n_e are also related to each other as $\nabla^2 \phi_s = en_e / \varepsilon_0$, where ε_0 is the permittivity of free space. From the above consideration, the Poisson-Boltzmann equation has been derived[10] for the equilibrium of one-species plasmas confined on magnetic surfaces, and Eq. (2) predicts that n_e and consequently ϕ_s need not be magnetic surface quantities when the electrostatic

[a)]Present address: Department of Electronics, Kyoto Institute of Technology, Matsugasaki Kyoto 606-8585, Japan. Electronic mail: himura@kit.ac.jp

force is not small compared to the pressure force. One of the key parameters of the theory is a/λ_D, where a and λ_D are a typical length of plasmas ($\sim$ average radius) and the Debye length, respectively. In fact, for $a/\lambda_D \sim 1-10$, it is expected[11] that ϕ_s and n_e vary significantly on magnetic surfaces.

In this paper, we report the first observation of variation in ϕ_s and n_e on magnetic surfaces of helical electron plasmas. The value of T_e reaches several hundred electron volts, depending on both the acceleration voltage V_{acc} of the injected electrons and the magnetic field strength B. The plasma is therefore hot. Values of a/λ_D of the plasmas are in the range between 1 and 10. By comparing two values of both ϕ_s and n_e on each magnetic surface, it is clearly shown that ϕ_s and n_e are not constant but vary significantly on magnetic surfaces. The observed variation of ϕ_s is of the order of T_e/e. Larger differences in ϕ_s are observed in the outer region of the plasmas where the value of ϕ_s decreases and stronger $\nabla_r \phi_s$ also exists. The difference in ϕ_s is significantly enhanced by larger V_{acc} of the injected electrons. These observations suggest a dependence of the ϕ_s variation on a/λ_d. The measured $n_e(z)$ shows that the contours of $n_e(z)$ tend to move towards the grounded chamber wall. The expected contours of ϕ_s near the magnetic axis R_{ax} seem to move upward with respect to contours of Ψ in the poloidal cross section shown in Fig. 1. That is, the ϕ_s contours move away from the grounded chamber wall. As the e-gun is inserted deeply to the plasma, values of ϕ_s decrease considerably, probably due to deformed equipotential surfaces and partially to short circuiting caused by the stainless-steel barrel of the e-gun. These results, therefore, clearly indicate the existence of plasma equilibria having nonconstant ϕ_s and n_e on magnetic surfaces.

II. APPARATUS

Experiments are conducted on a medium-sized stellarator machine called the Compact Helical System (CHS) (Ref. 12), which has major and averaged minor radii of 1 and 0.2 m, respectively. A schematic drawing of the three-dimensional structure of the CHS vacuum magnetic surfaces is shown in Fig. 1(a) and principal parameters of experiments are listed in Table I. A more detailed explanation of the experimental setup is found in Ref. 7. The magnetic field (henceforth, called B field) is static and the maximum value of B at R_{ax} is about 0.9 kG. Typical vacuum pressure of CHS is about 2×10^{-8} Torr. In order to produce electron plasmas we use a LaB_6 emitter as the cathode, and the e-gun with it is inserted horizontally along the r axis. Electrons can be launched out into the vacuum B field with V_{acc} up to ~ -1.2 kV. The emission beam current I_b is variable, but we have limited I_b to $\sim$0.1 A for the experiments presented here. The pulse width of I_b is also fixed at 40 ms. Two Langmuir emissive probes are used to measure ϕ_s and the probe current I_p in helical electron plasmas. To prevent short circuiting of ϕ_s across magnetic surfaces, both probe shafts are covered with quartz tubes; the outer diameter of the tubes is 6 mm. One probe is inserted horizontally along the r axis, and the other is installed vertically along the z axis. In the following discussion, we will refer to these probes as r probe and z probe, respectively. A vertically elongated cross section is defined as the origin for toroidal position $\varphi=0°$. The e-gun, r, and $z$probes are located at $\varphi=32.5°$, 157.5° (called the "5-O" cross section), and 232° (called the "6-U" cross section), respectively, where increasing toroidal angle is measured counterclockwise from above. Figure 1(b) shows the 6-U cross section of CHS with magnetic surfaces (solid red curves), where the z probe is located. Since the length of the z probe is about 60 cm, ϕ_s is measured at two different

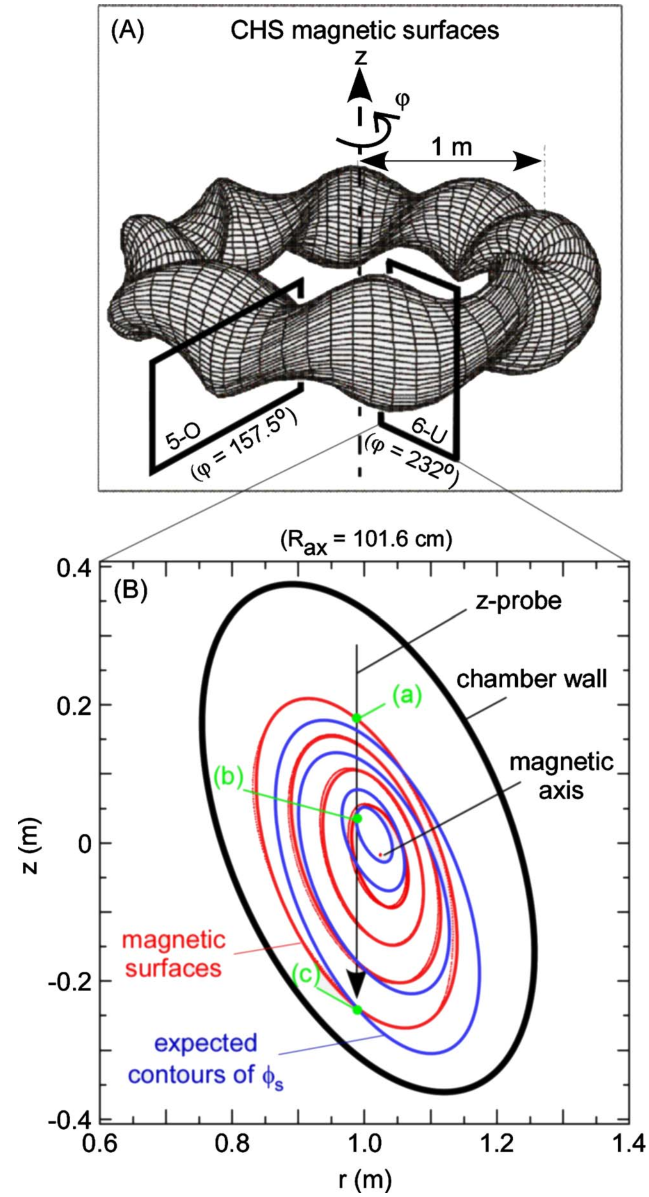

FIG. 1. (a) A schematic drawing of three-dimensional structure of the CHS vacuum magnetic surface. Two solid rectangles indicate the 6-U and the 5-O cross sections where the z probe and the r probe are installed, respectively. (b) The 6-U cross section. In this figure, the Poincare plots of 10 magnetic surfaces (red curves) and expected contours of space potential ϕ_s (blue curves) inferred from measured data [shown in Fig. 2(a)] are shown. The magnetic axis R_{ax} is at 101.6 cm. The z probe moves vertically. Since the length of the z probe is 60 cm, values of ϕ_s can be measured at two different points on each magnetic surface. Three measurement points labeled as (a), (b), and (c) correspond to the measurement points in Fig. 2 with the same symbols.

TABLE I. Principal parameters of helical nonneutral experiments on CHS.

CHS	Major radius	1 m
	Averaged minor radius	0.2 m
	Pole number	2
	Field period number	8
	Field strength on axis	<0.9 kG
Electron gun (e-gun)	Emission area	$\sim 1\ \mathrm{cm}^2$
	Acceleration voltage	>-1.2 kV
	Beam current	<0.1 A
	Beam density	$<1\times 10^{14}\ \mathrm{m}^{-3}$
Helical electron plasma for $V_{\mathrm{acc}}\sim 600$ V	Averaged volume density	$\sim 5\times 10^{13}\ \mathrm{m}^{-3}$
	Temperature	<170 eV
	Debye length	~ 2.6 cm
	Electron Larmor radius	<1.3 mm
	Maximum space potential	~ 690 V

points on a magnetic surface; one measurement point is in the $z>0$ region and the other is in the $z<0$ region, vice versa.

III. EXPERIMENTAL RESULTS

A. Injection of electrons from 1 cm outside LCFS

1. Space potential ϕ_s

The data plotted in Fig. 2(a) are $\phi_s(z)$ measured with the z probe using the high-impedance emissive method.[13] The horizontal axis is $\Psi^{1/2}$, where $\Psi^{1/2}=0$ and 1 correspond to the R_{ax} and LCFS,[7] respectively. In experiments presented here, R_{ax} is fixed at $r=101.6$ cm. Thus, magnetic surfaces containing plasma do not touch the grounded chamber wall. The z probe does not cross R_{ax}, being shifted about 4 cm inward from R_{ax}. Consequently, the lower limit of measurement points of $\phi_s(z)$ is $\Psi^{1/2}=0.3$ on this cross section. All data points plotted in Fig. 2(a) are averaged values of three different series of experiments. For each shot, the value of ϕ_s is determined by time averaging $\phi_s(t)$ in first 0.2–0.5 ms just after the signal curve has risen completely. For the data measured at $\Psi^{1/2}=0.9$, however, those are time averaged in first ~ 2 ms, because they take longer time to rise up. Error bars denote the maximum and minimum values of $\phi_s(t)$ during the time averaging period.

Differences between two values of ϕ_s at $z>0$ (henceforth ϕ_{s_u}) and ϕ_s at $z<0$ (henceforth ϕ_{s_d}) on each magnetic surface (at same value of $\Psi^{1/2}$) are observed. This means that ϕ_s is not constant on magnetic surfaces. As is shown from the data, the difference in ϕ_s becomes larger in the outer region of magnetic surfaces. Actually, the difference reaches about 120 V at $\Psi^{1/2}\sim 0.9$, while at $\Psi^{1/2}\sim 0.3$ the difference almost disappears. Also, one notes that there are two "*crossover*" points of the measured $\phi_s(z)$, which are at $\Psi^{1/2}\sim 0.3$ and 0.8. Inside $\Psi^{1/2}\sim 0.3$, ϕ_{s_u} seems to be somewhat smaller than ϕ_{s_d} or almost equal to it, while $\phi_{s\_u}>\phi_{s\_d}$ between the two crossover points. Outside $\Psi^{1/2}\sim 0.8$, the magnitude relation is flipped again, that is, $\phi_{s\_u}<\phi_{s\_d}$.

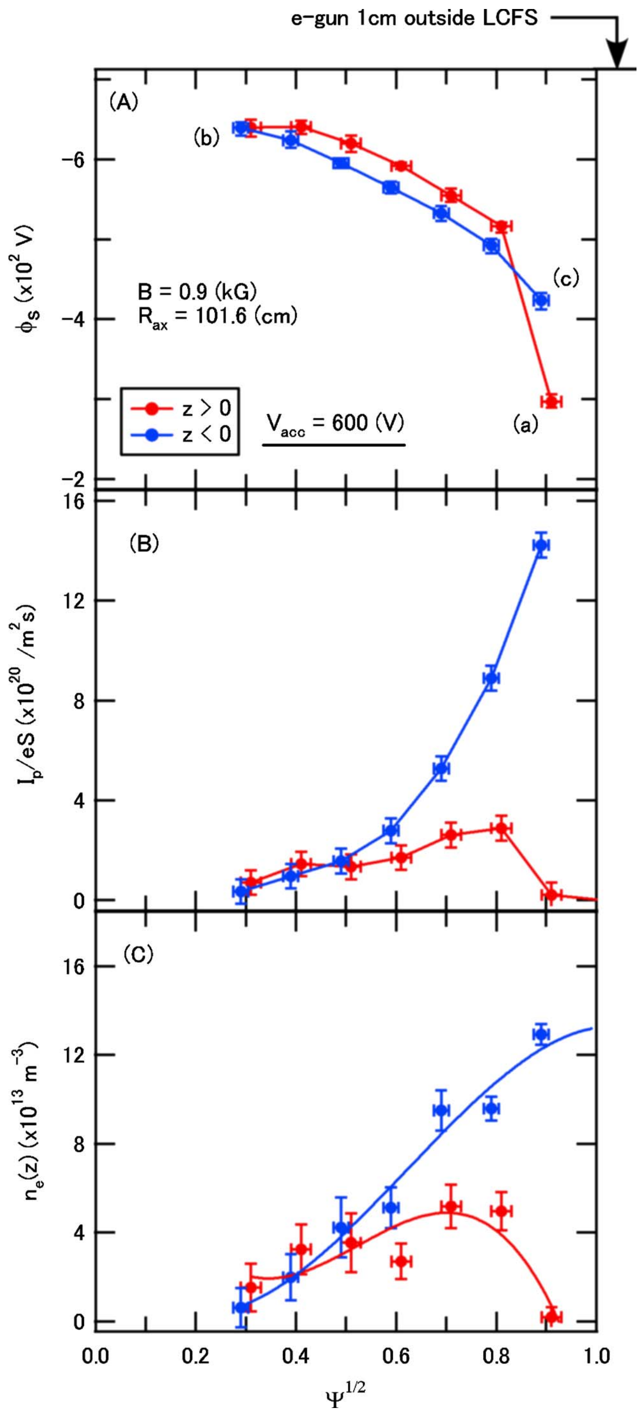

FIG. 2. Profiles of (a) space potential $\phi_s(z)$, (b) electron particle flux $\Gamma_e(z)$, and (c) electron density $n_e(z)$ measured at the 6-U cross section for the case of $V_{\mathrm{acc}}=-600$ V. The horizontal axis is the normalized minor radius. Three labels of (a), (b), and (c) correspond to those shown in Fig. 1. The position of the e-gun is at 1 cm outside the LCFS on a different poloidal cross section (see Ref. 8). Fitting curves on $n_e(z)$ are calculated using polynomial functions and put for the reader's convenience.

Meanwhile, at the 6-U cross section, the helical magnetic surfaces have been slightly shifted downward with respect to the center of the elliptic chamber wall [see, also, Fig. 1(b)]. The inferred contours of ϕ_s (equipotential surfaces) from the measured $\phi_s(z)$ are shifted upward inside $\Psi^{1/2}\sim 0.8$, while downward outside $\Psi^{1/2}\sim 0.8$, with respect to the contours of constant ψ (magnetic surfaces). The blue curves overwritten on the magnetic surfaces (red curves) in Fig. 1 are the inferred contours of ϕ_s (see, also, Fig. 2).

2. Electron density n_e

In this research, the current-voltage (I_e-V_p) characteristics are also measured on each magnetic surface with the same emissive probes that are used to measure ϕ_s. For this measurement, the impedance of the probe is low (330 Ω) so as to obtain the electron current I_e that flows from the plasma to the probe. From the I_e-V_p characteristic curve, we have determined the electron temperature T_e, as will be described. Then, assuming I_e ($\sim e n_e v_{th} S$) at $V_p = \phi_s$, the electron particle flux Γ_e is obtained as $\Gamma_e \sim I_e / eS$, as shown in Fig. 2(b). Subsequently, the electron density n_e is calculated. Here, v_{th} is electron thermal speed and S is the probe area. The bias voltage V_p is tuned in ϕ_s measured just before the current measurement to alleviate an experimental error. All other contributions to I_e except v_{th} are ignored, because v_{th} dominates the electron flux to the probe.

Figure 2(c) shows $n_e(z)$ for $B = 0.9$ kG and $V_{\mathrm{acc}} = -600$ V; values of n_e measured at $z > 0$ (henceforth n_{e_u}) and $z < 0$ (henceforth n_{e_d}) are identified by red and blue circles, respectively. Substantial nonuniformity on each magnetic surface is clearly observed. Fitting curves on $n_e(z)$ are calculated using polynomial functions and put for the reader's convenience. Another significant point is that $n_e(z)$ has only one crossover point that appears at $\Psi^{1/2} \sim 0.4$. Also, n_{e_d} is always larger than n_{e_u} outside $\Psi^{1/2} \sim 0.4$. This result means that electrons tend to move towards the grounded chamber wall.

B. Injection of electrons from $\Psi^{1/2} \sim 0.9$

The above variation of ϕ_s and n_e along with the crossover is still observed for the case where the e-gun is inserted into closed magnetic surfaces by 2 cm from the LCFS to $\Psi^{1/2} \sim 0.9$. Figures 3(a)–3(c) show $\phi_s(z)$, $\Gamma_e(z)$, and $n_e(z)$, respectively. However, for this case, only does one crossover of $\phi_s(z)$ appear. Furthermore, the crossover point seems to shift to $\Psi^{1/2} \sim 0.6$. Such a shift cannot be observed clearly in $n_e(z)$ shown in Fig. 3(b), on the other hand. These observations indicate that $\phi_s(z)$ changes more sensitively in response to the location of the e-gun. Regarding the gradient of the measured $\phi_s(z)$ and $n_e(z)$, it is clearly seen that for this case both $\phi_s(z)$ and $n_e(z)$ become more steep outside $\Psi^{1/2} \sim 0.7$, probably due to an effect caused by the e-gun insertion, as will be discussed.

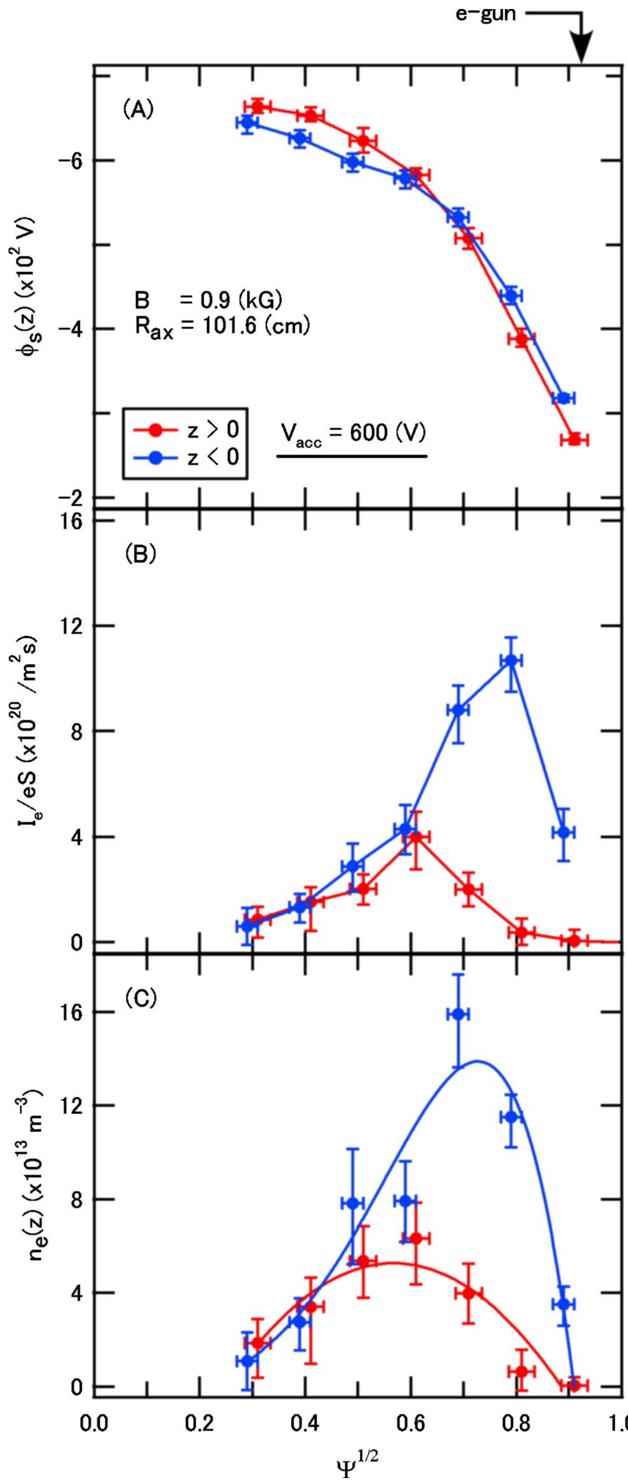

FIG. 3. Profiles of (a) $\phi_s(z)$, (b) $\Gamma_e(z)$, and (c) $n_e(z)$ obtained with the same experimental settings as those in Fig. 2 except the e-gun position. For this case, the e-gun is inserted by 3 cm (from the LCFS to $\Psi^{1/2} \sim 0.9$).

C. Dependence on V_{acc}

In experiments, we have also changed the acceleration voltage V_{acc} of the electron injection. Two profiles of $\phi_s(z)$, identified with solid circles in Fig. 4, are obtained for the case of $V_{\mathrm{acc}} = -1$ kV. As recognized, the difference in ϕ_s becomes larger. However, one notes that for this case the magnitude relation between ϕ_{s_u} and ϕ_{s_d} seems to be changed, which turns to be $\phi_{s\_u} > \phi_{s\_d}$ inside $\Psi^{1/2} \sim 0.7$. Although not presented here, for $V_{\mathrm{acc}} = -300$ V, the difference in ϕ_s has becomes smaller at all measurement points, compared with those for $V_{\mathrm{acc}} = -600$ V.

D. Effect of probing

As described above, $\phi_s(z)$ has been changed by the e-gun insertion (see, also, Figs. 2 and 3). This implies that

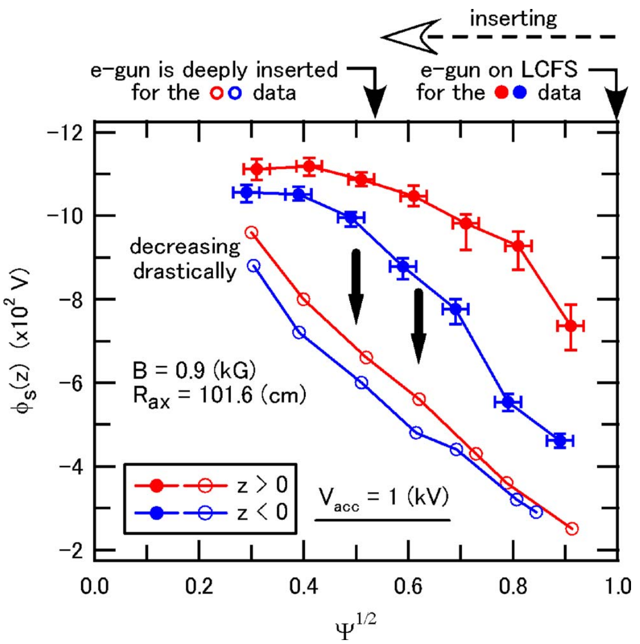

FIG. 4. Profiles of $\phi_s(z)$ for cases where $V_{\rm acc}=-1$ kV and the e-gun is located at $\Psi^{1/2}\sim 1$ (solid circles). Degradation of $\phi_s(z)$, when the e-gun is inserted deeply at $\Psi^{1/2}\sim 0.5$, is also presented (outline circles).

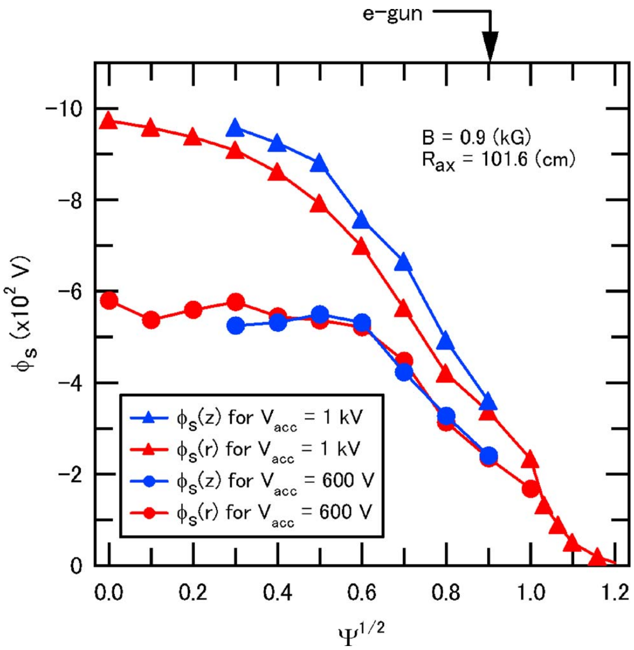

FIG. 5. Typical radial profiles $\phi_s(r)$ measured at the 5-O cross section along with $\phi_s(z)$. The corresponding combination of $\phi_s(r)$ and $\phi_s(z)$ identified with same symbols are obtained simultaneously: $V_{\rm acc}=-600$ V (circles) and -1 kV (triangles).

the equilibrium of the plasma would be perturbed more, when the e-gun is inserted deeply into the plasma confinement region. In order to check it also for $V_{\rm acc}=1$ kV experimentally, we have measured $\phi_s(z)$ when the e-gun is set at $\Psi^{1/2}\sim 0.5$. As seen from the outline circles plotted in Fig. 4, values of ϕ_s decrease significantly at all measurement points. Also, the difference in ϕ_s almost disappears on all magnetic surfaces outside $\Psi^{1/2}\sim 0.7$.

Since the $\phi_s(z)$ measurements are performed by insertion of the z probe all the way to point (c) in Fig. 1, the question may be asked on how the probe insertion affects the measured ϕ_s. To answer it experimentally, we have measured $\phi_s(z)$ by changing the position of the r probe at the 5-O cross section [see, also, Fig. 1(a)]. Figure 5 shows typical profiles of both $\phi_s(z)$ and $\phi_s(r)$, which are measured simultaneously. One notes that $\phi_s(r)$ is obtained outside $R_{\rm ax}$ ($r>101.6$ cm), while $\phi_s(z)$ is taken below $R_{\rm ax}$ ($z<0$), that is, equivalently ϕ_{s_d}. These are thus helically symmetric with respect to $R_{\rm ax}$. Comparing $\phi_s(z)$ in Fig. 5 with those (being measured without the r probe insertion) in Figs. 2 and 3, no significant degradation in $\phi_s(z)$ is found even when both the z and r probes are fully inserted into the magnetic surfaces to measure ϕ_s near $R_{\rm ax}$. From these checks, we have concluded that the probing itself never causes the observed variation in ϕ_s on magnetic surfaces.

By the way, for the $V_{\rm acc}=-600$ V case, the two profiles of $\phi_s(r)$ and $\phi_s(z)$ in Fig. 5 seem to agree well, suggesting the existence of little toroidal electric field E_t on the magnetic surfaces between the 5-O and 6-U cross section, while considerable E_t seems to exist between the two cross sections for $V_{\rm acc}=-1$ kV. These tendencies may also reflect the thermal effects on the force balance along magnetic field lines. The variation of ϕ_s in toroidal direction is now investigated and will be reported elsewhere.

IV. DISCUSSION

First, effects of the probing and the e-gun insertion on the observed nonconstant ϕ_s and n_e are considered. As seen in Fig. 5, no probing caused the nonconstant ϕ_s on magnetic surfaces. This is probably due to the narrower shaft (the diameter is 6 mm) of the probe insulated with a quartz tube, preventing electrical short circuiting. On the other hand, the e-gun insertion resulted in remarkable degradation of the measured ϕ_s (see, also, Fig. 4). This should be caused by the barrel of the e-gun. Its diameter is about 25 mm, which is hardly slender enough. Furthermore, the barrel is made of stainless steel and connected to ground electrically. As a result, it would bring in deformed equipotential surfaces and cause partial short circuiting on the surface of the barrel, thus destroying the plasma equilibrium. In fact, as seen from the data outside $\Psi^{1/2}\sim 0.7$, the red and blue outline circles seem to agree well on every magnetic surface, suggesting that ϕ_s is constant on the magnetic surfaces. The reason why ϕ_s is not completely down to zero, but finite, is unclear, possibly due to the continuous injection of electrons. However, these observations represent an additional piece of evidence, supporting the conclusion that variation of ϕ_s in equilibrium state exists in the unperturbed equilibrium.

The result that the difference in two values of ϕ_s measured on the same magnetic surface grows with increasing $V_{\rm acc}$ suggests thermal motion of the electrons as a possible mechanism. In fact, by a dimensional analysis of Eq. (2), the variation of ϕ_s could be on the same order of T_e/e. In Fig. 6, the measured $T_e(z)$ for $V_{\rm acc}=-600$ V and $B=0.9$ kG is described. As seen from the data, values of T_e are in the range between 40 and 170 eV. The order of this T_e corresponds approximately with the observed variations of ϕ_s, which is

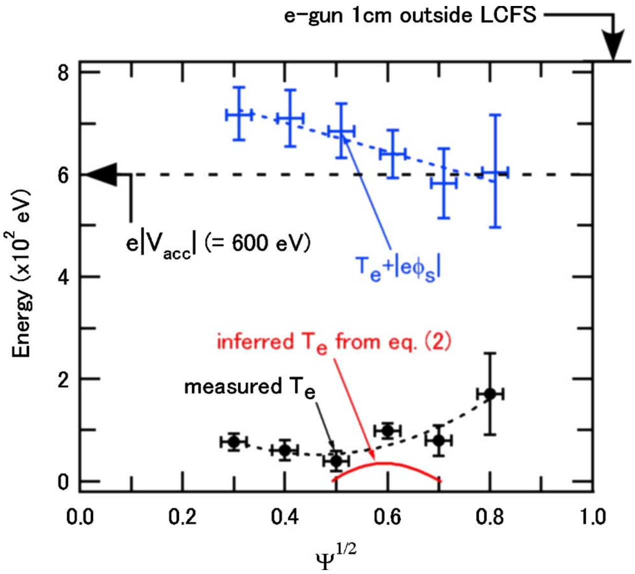

FIG. 6. A typical profile of electron temperature $T_e(z)$ for B=0.9 kG and $V_{\rm acc}$=−600 V (black circles). The red curve shows the theoretical T_e inferred from Eq. (2). Data identified with blue dots indicate the sums of thermal and potential energies (approximately, the total energy of a single electron) calculated from the experimental values. As recognized, they do not exactly agree with the initial energy of an electron.

$\lesssim$120 V (see, also, Fig. 2). Similar conclusions also held for the $V_{\rm acc}$=−1 kV case in which $T_e \lesssim 200$ eV and the difference in ϕ_s were not more than 370 V.

However, there is somewhat a discrepancy between the measured T_e and the theory. Since $n_e(z)$ and $\phi_s(z)$ are measured, the theoretical $T_e(z)$ can be roughly calculated from Eq. (2), assuming that $T_e(z) \sim (1/2)(n_{e\_u}+n_{e\_d}) \times(\phi_{s\_u}-\phi_{s\_d})/(n_{e\_u}-n_{e\_d})$, where $(1/2)(n_{e\_u}+n_{e\_d})$ approximates n_e in Eq. (2). In Fig. 6, the calculated $T_e(z)$ using the data in Fig. 2 is identified with a red curve. Here, the result is presented only for $0.5<\Psi^{1/2}<0.7$, because there are crossover points in both $n_e(z)$ and $\phi_s(z)$, which make the value of T_e infinity and zero, respectively. It is recognized that the theoretical $T_e(z)$ is smaller than the measured one. This might be attributed to either a bit of inaccuracy of the T_e measurement using the I_e-V_p characteristic curve or insufficient thermalization of the injected electrons. In fact, as seen from the data of the total energy of a single electron $(e|V_{\rm acc}|=T_e+|e\phi_s|+E_{\rm flow}\simeq T_e+|e\phi_s|)$, values of $T_e+|e\phi_s|$ are not exactly equal to $e|V_{\rm acc}|$, in particular, inside $\Psi^{1/2}=0.6$ it is more apparent. Further consideration is thus required about the T_e measurement.

Regarding the variations of both ϕ_s and n_e, the volume-averaged plasma density $\langle n_e\rangle$ is about 5×10^{13} m^{-3} for the case[15] of $V_{\rm acc}$=−600 V and B=0.9 kG (Figs. 2 and 3). Thus, the typical volume-averaged value of a/λ_D is about 5. For this case, the observed nonconstant ϕ_s on magnetic surfaces is certainly expected.[11] The findings that both ϕ_s and n_e vary more strongly on outer magnetic surfaces than on internal surfaces, and that ϕ_s on the part of the surface near the grounded vacuum chamber (ϕ_{s_d}) is less negative than ϕ_s on the part of the surface further away from the vacuum chamber (ϕ_{s_u}) for $V_{\rm acc}$=−1 kV (see, also, Fig. 4), are in agreement with what is seen in numerical solutions to the equilibrium equation.[11] In fact, recent numerical calculations[16] of the CHS equilibrium qualitatively reproduce the effects reported here.

The reason why the electrons tend to move downward can be also understood from the shift of $\phi_s(z)$ qualitatively. As explained, the envisioned contours of ϕ_s have shifted upward with respect to the contours of constant ψ (see, also, Fig. 1). In this case, the corresponding (global) direction of $E_{//}$ in the poloidal cross section results in the upward direction as well. Therefore, electrons are forced toward the downward side $(z<0)$ of the magnetic surfaces. In fact, this seems also to be consistent with the stability analysis[14] for nonneutral plasmas confined in magnetic surfaces. However, for the $V_{\rm acc}$=−600 V case, ϕ_{s_d} turned to be more negative at $\Psi^{1/2}\sim0.7-0.9$ than ϕ_{s_u} (see, also, Figs. 2 and 3), which was not observed for the $V_{\rm acc}$=−1 kV case. The reason is so far unknown. One of the possible reasons to explain the observation is the effect of self-electric potential of the excess beam electrons circulating near the LCFS. A numerical calculation of ϕ_s including the self-electric potential may answer the question.

Since the observed variation of ϕ_s increases with larger $V_{\rm acc}$, one may ask how $V_{\rm acc}$ is related to the observation. As explained, $V_{\rm acc}$ has been varied over the range between −0.3 and −1 kV. Thus, the corresponding (directed) speed of injected electrons v_0 $(\sim\sqrt{2eV_{\rm acc}/m_e})$ is calculated to be $\sim1\times10^7$ m/s for $V_{\rm acc}$=−300 V and 1.9×10^7 m/s for $V_{\rm acc}$=−1 kV, which varies by only a factor of 2. It is not large enough to explain the observed difference in ϕ_s.

Finally, we should mention the effect of magnetic islands on the observed ϕ_s variation on magnetic surfaces, because data are obtained in helical magnetic surfaces. A magnetic field mapping experiment[17] has identified magnetic islands on the m=2, 3, and n=1 major rational surfaces on CHS, where m and n denote the poloidal and toroidal mode numbers, respectively. Since the width of the $n/m=1/2$ island is about 2.5 cm for the case where $B\simeq$at $R_{\rm ax}$ is 0.9 kG, the islands probably influence the local structure of ϕ_s around the rational surfaces. However, as already shown in Figs. 2–4, the observed variation of ϕ_s has not been limited near the rational surfaces, but extends over the whole range of magnetic surfaces. Therefore, it is considered that the magnetic islands are not the reason for the observed variation in ϕ_s on magnetic surfaces.

ACKNOWLEDGMENTS

The authors are grateful to the CNT group at Columbia University, especially T. Pedersen, R. Lefrancois, and A. Boozer for fruitful discussions and comments. This work is performed under the auspices of the NIFS CHS Research Collaboration.

[1] J. Wesson, *Tokamaks*, 2nd ed. (Oxford University Press, New York, 1997), p. 109.
[2] M. Wakatani, *Stellarator and Heliotron Devices* (Oxford University Press, New York, 1998), p. 8.
[3] R. C. Davidson, *Physics of Nonneutral Plasmas* (Addison-Wesley, Redwood City, CA, 1990), p. 42.

[4] H. Himura, Z. Yoshida, Y. Ogawa *et al.*, *Fusion Energy 2000* (International Atomic Energy Agency, Vienna, 2001), ICP/14.
[5] Z. Yoshida, Y. Ogawa, J. Morikawa *et al.*, in *Non-neutral Plasma Physics III*, AIP Conf. Proc. No. 498, edited by J. J. Volinger, R. L. Spencer, and R. C. Davidson (AIP, Melville, NY, 1999) p. 397.
[6] B. Ghaffari and R. S. Conti, Phys. Rev. Lett. **75**, 3118 (1995).
[7] H. Himura, H. Wakabayashi, M. Fukao, M. Isobe, S. Okamura, and H. Yamada, IEEE Trans. Plasma Sci. **32**, 510 (2004); H. Himura, H. Wakabayashi, M. Fukao *et al.*, Phys. Plasmas **11**, 492 (2004).
[8] J. P. Kremer, T. Sunn Pedersen, R. G. Lefrancois, and Q. Marksteiner, Phys. Rev. Lett. **97**, 095003 (2006).
[9] M. R. Stoneking, M. A. Growdon, M. L. Milne, and R. T. Peterson, Phys. Rev. Lett. **92**, 095003 (2004).
[10] T. S. Pedersen and A. H. Boozer, Phys. Rev. Lett. **88**, 205002 (2002).
[11] T. S. Pedersen, Phys. Plasmas **10**, 334 (2003); R. G. Lefrancois, T. S. Pedersen, A. H. Boozer, and J. P. Kremer, Phys. Plasmas **12**, 072105 (2005).
[12] K. Matsuoka, R. Akiyama, A. Fujisawa *et al.*, Plasma Phys. Controlled Fusion **42**, 1145 (2000).
[13] H. Himura, M. Fukao, H. Wakabayashi, and Z. Yoshida, Rev. Sci. Instrum. **74**, 4658 (2003).
[14] A. H. Boozer, Phys. Plasmas **11**, 4709 (2004).
[15] Because the e-gun is located not in the stochastic magnetic region but near the outer edge of closed magnetic surfaces in the presented experiments, thus higher values of n_e than previous data published in Ref. 7 are obtained.
[16] R. G. Lefrancois, private communication (2006).
[17] H. Yamada, K. Matsuoka, S. Okamura *et al.*, Rev. Sci. Instrum. **61**, 686 (1990).